JOURNAL OF MATERIALS SCIENCE **37** (2002) 3141 – 3147

Stereolithography of structural complex ceramic parts

T. CHARTIER
SPCTS, UMR CNRS 6638, ENSCI, 47/73 Avenue Albert Thomas, 87065 Limoges, France
E-mail: t.chartier@ensci.fr

C. CHAPUT, F. DOREAU, M. LOISEAU
CTTC, Ester Technopole, 87069 Limoges, France

A cost-effective method of complex ceramic parts manufacturing using stereolithography has been developed. The process consists in fabricating ceramic pieces by laser polymerization of an UV curable monomeric system, subsequent removal of organic components and sintering. Highly concentrated suspensions of well dispersed ceramic particles (up to 60 vol%) in a reactive acrylic monomer, with a suitable rheological behaviour for the spreading of thin layers (down to 25 μm) were defined. Adequate cured depth (higher than 200 μm) is obtained even at high scanning speeds. Nevertheless, a compromise has to be found between the cured depth and the cured width to improve the dimensional resolution. The dimensional resolution reached on alumina partterns is about 200 μm with an energy density of 0.05 J $\cdot$ cm^{-2}.

1. Introduction

Most of advanced ceramic processing techniques requires the use of tooling (dies, mould. . .) which are costly and take time to fabricate. In particular, injection moulding, largely used for the production of complex ceramic parts with high dimensional tolerances, requires an expensive mould, that makes this technique not adapted for the low mass production, and of course, for the fabrication of prototypes. In an other hand, when high level of complexity is required, it could be necessary to machine sintered ceramic parts with diamond tools. This type of machining could also be a route for production of unitary part, but the main drawbacks are, (i) a high cost linked to the time and to the use of diamond tools and, (ii) the introduction of defects due to the brittle nature of ceramics.

Over about fifteen years, many freeform processing methods of 3D ceramic parts without moulds or tooling have been developed, for instance selective laser sintering, three dimensional printing, fused deposition modelling, laminated object manufacturing and tape casting techniques.

The stereolithography method, which is largely used for the fabrication of three dimensional polymer parts, has been adapted to the process of 3D ceramic pieces with final properties (mechanical, thermal, electrical. . .) close to those obtained by classical processing techniques [1–6]. Stereolithography involved polymerization of a reactive system, generally based on acrylate or epoxy monomers, by a space resolved laser. The main applications of the fabrication, by stereolithography, of ceramic parts should be medical implants, direct fabrication of refractory moulds and cores or, of prototypes prior to defining an expensive mould of injection moulding.

This paper describes the fabrication of complex ceramic parts by stereolithography, removal of the polymer and sintering. A particular attention is paid to the influence of exposure conditions, powder characteristics (nature, particle size) and of the formulation of the reactive system (photoinitiator concentration, nature of the curable monomer) on the cured depth and width and on the dimensional resolution. Examples of sintered alumina parts with their characteristics are presented.

2. Experimental procedure

2.1. Starting materials

In order to evaluate the influence of the particle size, alumina powders with various particle sizes were used. Zircon and silica powders were also used to study the influence of the refractive index difference between the monomer and the ceramic material. Main characteristics of the powders used are given in Table I. In the same respect, two monomers (acrylates) were used (Table I). Adapted dispersants, which act both by electrostatic and steric repulsion, were used according to the nature of the powder. A thickener confers a high yield value to the paste to prevent settling of particles and to support the piece during fabrication. The photoinitiator absorbs in the range of the UV laser emission (Irgacure 651, Ciba, Switzerland).

2.2. Preparation of the suspensions

The photoinitiator, the dispersant and the thickener were first dissolved in the monomer, then the ceramic powder was added. Suspensions containing 50 to 60 vol% powder, were milled during 30 min. to break down the agglomerates and to achieve a good homogeneity. The rheological behaviour was optimised to

TABLE I Mean particle size and refractive index of powders used and refractive index of the two monomers used

Starting material	Grade	Supplier	d_{50} (μm)	Refractive index
Alumina	CT3000SG	AlCoA, USA	0.8	1.70
Alumina	CT1200SG	AlCoA, USA	1.5	1.70
Alumina	615-10	Nabaltec, Germany	2.9	1.70
Alumina	AC34	Péchiney, France	4.4	1.70
Zircon	Remet FG	Remet, USA	4.2	1.85
Silica	C600	Sifraco, France	3.5	1.50
Monomer 1				1.54
Monomer 2				1.47

allow suitable layer spreading and to achieve homogeneous green microstructure.

2.3. Fabrication of green ceramic pieces by stereolithography

The ceramic paste is introduced in a piston which deliver a controlled quantity on the working area. Homogeneous layers, with different thicknesses (down to 25 μm) and smooth surfaces were spread by means of a specific device before polymerization. Contrary to classical stereolithography equipments, where a fluid monomer is required, the machine uses a paste with a high viscosity, thus avoiding the use of a container.

Using CAD information, laser beam radiation (Arion laser, Coherent, $\lambda = 351$–364 nm), focused on the top surface of the deposited paste, was deflected by galvanometric mirrors. When a layer of the part was performed, the deposition of a subsequent layer of paste on the already polymerized part allowed the continuation of the manufacturing process. This procedure was repeated until the polymer part was built. Green parts are then cleaned from non-polymerized suspension using a solvent.

2.4. Binder removal and sintering

Alumina (CT1200SG grade, $d_{50} = 1.5$ μm) green samples were debinded with a heating rate of $1°C \cdot min^{-1}$ up to 120°C, then of $0.2°C \cdot min^{-1}$ up to 550°C with a plateau of 3 h. The polymeric phase was then completely removed. The parts were finally sintered with a heating rate of $5°C \cdot min^{-1}$ up to 1700°C with a 1.5 h plateau. The density of sintered pieces was 97% of the theoretical density.

2.5. Characterisation

Rheological measurements were performed with a controlled stress rheometer (RS150, HAAKE, Germany) using a cone-plane configuration.

The reactive system has to verify two main requirements, (i) the cured depth must be high enough to avoid an excessive time of fabrication and, (ii) the cured width must be low to ensure a good resolution. In this respect, cured depth and width were measured on small polymerized lines cured in one layer by one scanning of the laser beam. The brittle polymerized lines were included in an epoxy resin in order to cut sections for observation. The values of depth and width correspond to the average of four measurements.

The flexural strength of as-sintered and polished alumina bars ($3.5 \times 5.5 \times 40$ mm^3) was measured by three-point bend tests (average of five values).

3. Results and discussion

3.1. Rheological behaviour

A rheological behaviour adapted to the principle of the specific stereolithography technique used is required. A typical shear thinning behaviour is presented in Fig. 1 in the case of the CT1200SG alumina paste (60 vol%). The high yield value (1200 Pa) allows to prevent non-insulated surfaces from flowing during the building of the piece and then to support it. The shear thinning behaviour allows spreading of homogeneous layers with a thickness as low as 25 μm. At a shear rate of 100 s^{-1}, corresponding to the minimum value generated by the spreading device, the measured viscosity is 110 $Pa \cdot s$, compared to 3500 $Pa \cdot s$ at rest.

3.2. Depth and width of photopolymerization

A first objective is to reduce the time of fabrication of pieces, then to use a high scanning speed while maintaining a sufficient cured depth. A second objective is to obtain a good dimensional resolution, and then to control the width of polymerization.

The evolution of the cured depth and width, in function of the density of energy, for different natures of powder, are given in Fig. 2.

It is interesting to note that a depth of polymerization from 180 to 600 μm, for a 50 vol% loaded system, can be achieved using a high scanning speed ($1\ m \cdot s^{-1}$), corresponding to $DE = 0.32\ J \cdot cm^{-2}$.

The cured depth (E_p) depends on the density of energy (DE) transmitted to the paste, on the depth of penetration of the beam (D_p), and on the critical density of energy (DE_c) that represents the smallest DE for which polymerization occurs:

$$E_p = D_p \ln\left(\frac{DE}{DE_c}\right) \quad (1)$$

The density of energy DE is function of the power of irradiation P, of the scanning speed v and of the radius

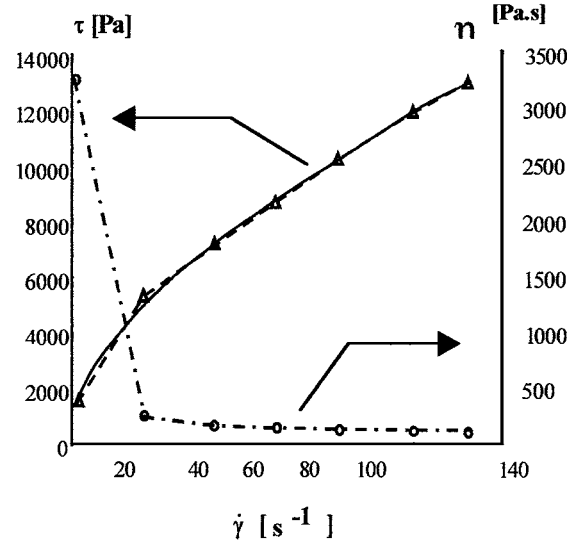

Figure 1 Rheological behaviour of the alumina paste (60 vol%).

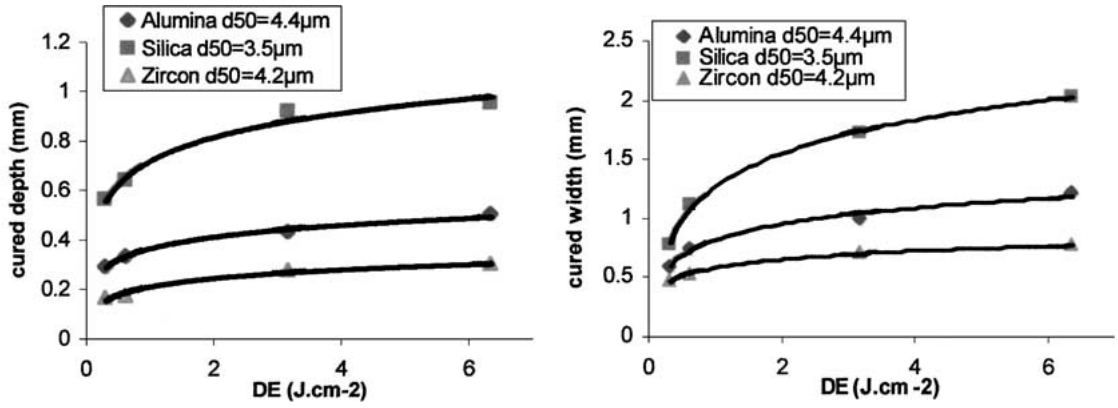

Figure 2 Cured depth and width versus density of energy (*DE*) for the three powders tested with a similar particle size (50 vol%–0.5 wt% photoinitiator).

of the laser spot w_0 (60 μm) on the working surface:

$$DE = \frac{2 \cdot P}{\pi \cdot w_0 \cdot v} \tag{2}$$

The depth of penetration D_p is a function of the mean diameter d_{50} and of the volume fraction ϕ of the powder, and function of a factor Q, representing the capability of a matter to diffuse a radiation:

$$D_p = \frac{2}{3} \frac{d_{50}}{Q \cdot \phi} \tag{3}$$

Griffith and Halloran [3], proposed an experimental law that relates the factor Q to the interparticule distance h, to the wavelength λ of irradiation and to the square of the difference between the refractive index of the powder and of the monomer, such as $\Delta n^2 = (n_{powder} - n_{resin})^2$:

$$Q = \frac{h}{\lambda} \cdot \Delta n^2 \tag{4}$$

The width of polymerization is always larger than the laser beam diameter, suggesting scattering phenomena due to the presence of ceramic particles. In the example of the CT1200SG alumina, for a cured depth of 300 μm ($DE = 0.32$ J $\cdot$ cm^{-2}), the width of polymerization (about 600 μm) is 5 times larger than the laser beam diameter.

The classical theories of scattering (Rayleigh, Gans, Mie) are verified for diluted system ($\phi < 0.1$), but are not valid for high loading values and cannot be applied to concentrated systems. Scattering behaviour of high loaded systems is still misunderstood. Nevertheless, an empirical expression of the width of photopolymerization W_p was proposed by Hinczewski [7]:

$$W_p = \sqrt{2} \cdot w_e \cdot \sqrt{\ln\left(\frac{DE}{DE'_c}\right)} \tag{5}$$

where w_e is an equivalent diameter, larger than the diameter of the laser beam, and DE'_c is the critical density of energy (different from DE_c—Equation 1). The equivalent diameter w_e mainly depends on the characteristics of the paste (initiator and powder concentrations, monomer and powder nature). But there is no satisfying law, experimental or theoretical, that can correctly predict or correlate the value of w_e according to the parameters representative of the composition.

Logarithmic behaviour of cured depth and width is observed with the density of energy whatever the nature of the powder (Fig. 2) that is in agreement with Equations 1 and 5. Calculated values of D_p, DE_c, Q, w_e and DE'_c are given in Table II.

The depth of penetration of the laser beam (D_p) as well as the equivalent diameter for width (w_e) are decreasing with increasing values of the refractive index difference, with a higher value for silica, than for alumina and zircon. The factor Q is increasing with the refractive index difference, that is in agreement with Equation 4, but the linear law between Q and Δn^2 is not verified in our case for constant h and λ values. The variation of critical values of density of energy, DE_c and DE'_c, in functiun of the refractive index difference are difficult to explain.

A high cured depth requires a high density of energy whereas a high resolution requires a low density of energy. Then, a compromise has to be found, firstly to reduce the time of fabrication of pieces, and secondly to obtain a good dimensional resolution. In this context, the cured cross-sectional dimensions have been studied in function of several parameters, such as the photoinitiator concentration, the powder concentration, the mean particle diameter and the nature of powder.

3.3. Influence of the photoinitiator concentration

In order to evaluate the influence of the photoinitiator concentration, cross-section dimensions of cured lines polymerized with pastes prepared with the three powders tested, i.e., alumina, zirconia and silica are

TABLE II Calculated values of D_p, DE_c, Q and w_e, using Equations 1, 3 and 5

Nature of powder	d_{50} (μm)	$\Delta n = (n_{powder} - n_{resin})$	D_p (μm)	DE_c (mJ $\cdot$ cm^{-2})	Q	w_e (μm)	DE'_c (mJ $\cdot$ cm^{-2})
Silica	3.5	0.03	140	6.15	0.033	410	46.1
Alumina	4.4	0.23	68	4.80	0.086	196	15.5
Zircon	4.2	0.38	50	14.94	0.112	102	3.3

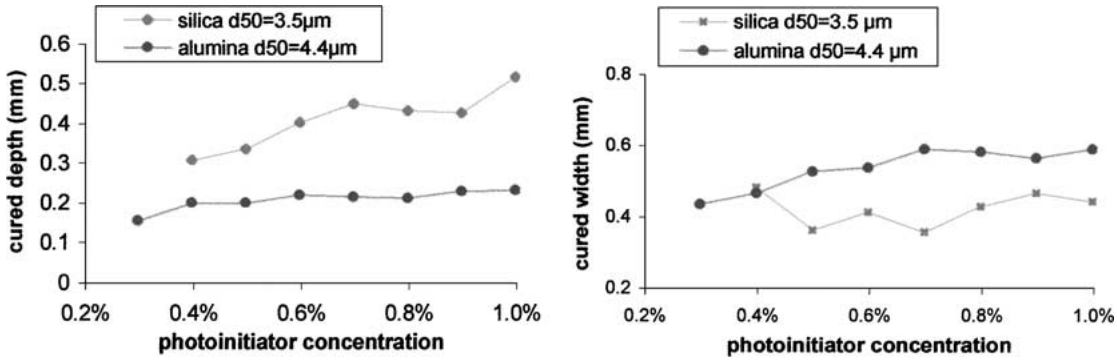

Figure 3 Influence of the photoinitiator concentration on cured depth and width for C600 silica and AC34 alumina powders ($DE = 3.18\ J \cdot cm^{-2}$–50 vol%).

measured for different concentrations of photoinitiator, ranging from 0.3 to 1 wt% based on the monomer weight. Two powder concentration, i.e., 50 and 60 wt% were tested (Fig. 3). In the range of the concentration tested, no significant influence of the photoinitiator concentration was observed. Nevertheless, a too high photoinitiator concentration (>2 wt%) led to a loose of reactivity (the laser beam is highly absorbed by the quickly polymerized surface).

3.4. Influence of the powder concentration

Cured depth and width for two different powders (AC34 alumina and C600 silica) are measured for three powder concentrations (25, 40 and 60 vol%) and three densities of energy (Fig. 4). The photoinitiator concentration for all compositions is 0.5 wt%.

Cured depth and width are decreasing as powder concentration, which is a non-reactive phase, is increasing. Cured depth variations with the powder concentration is well described by a "power" law tendency, with exponent values of about −0.9 for the two tested powders, that is in rather good agreement with Equation 3. Cured width behaviour versus powder concentration could also be fitted with a power law, with an exponent close to −1, similar to that obtained for the cured depth.

3.5. Influence of the mean diameter of particles

The influence of the average diameter of particles was evaluated by measuring cured depth and width for four alumina powders with different mean diameters

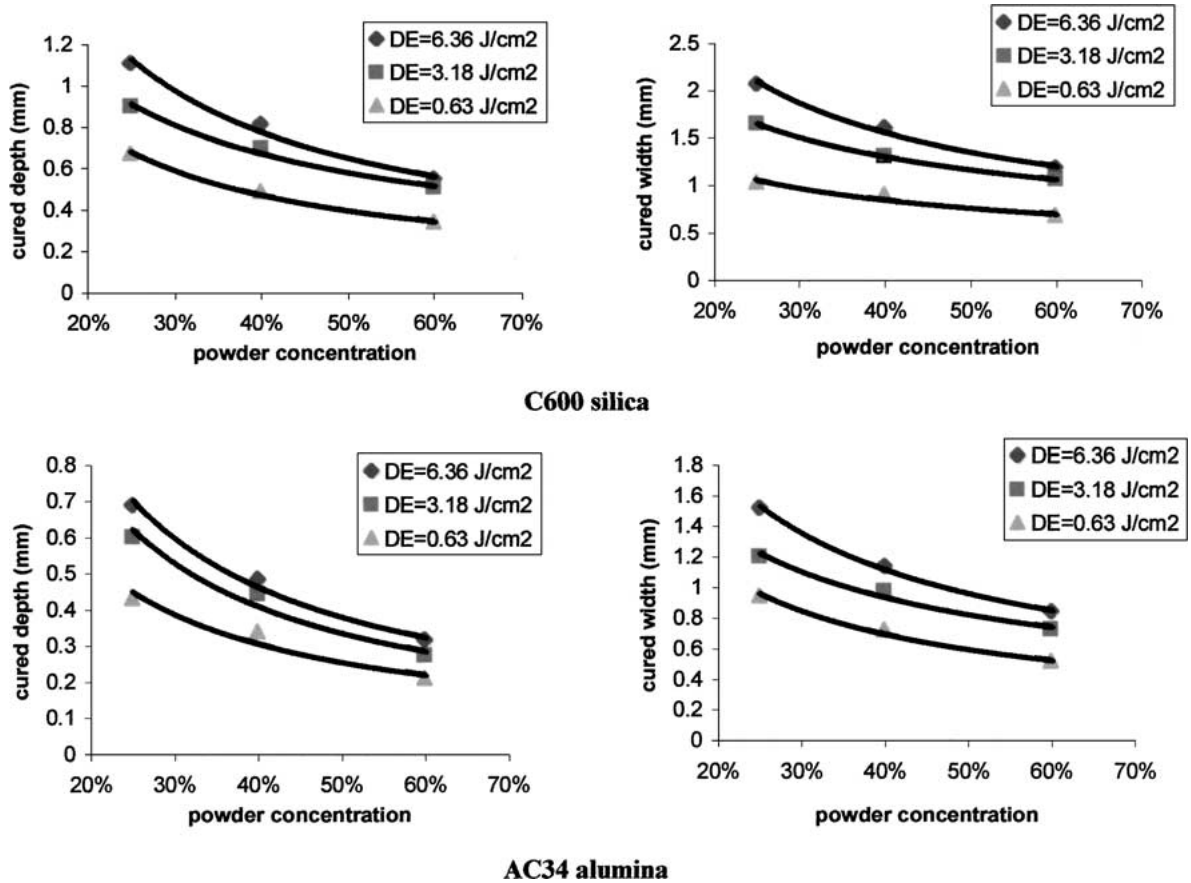

Figure 4 Cured depth and width for AC34 alumina ($d_{50} = 4.4\ \mu m$) and C600 silica ($d_{50} = 3.5\ \mu m$) powders in function of the powder concentration.

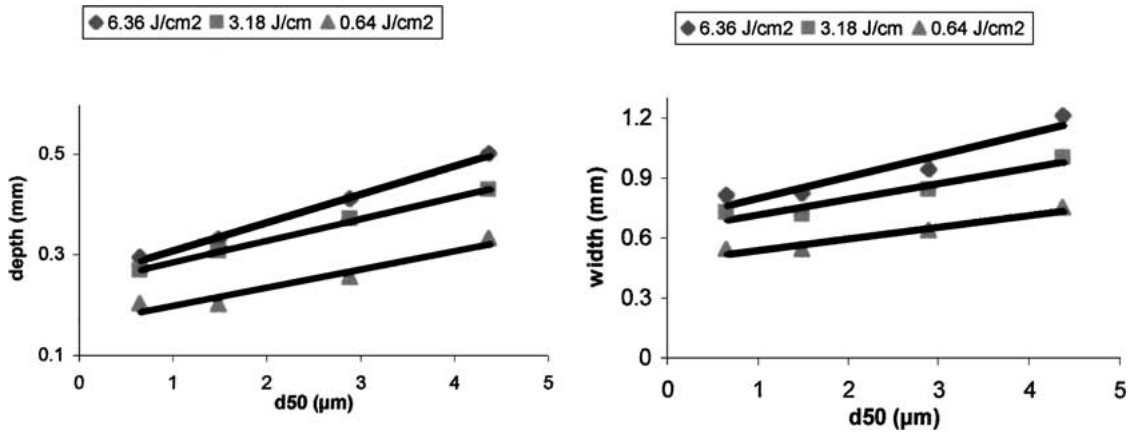

Figure 5 Cured width and depth in function of the mean diameter of alumina powder for three densities of energy (50 vol%–0.5 wt% photoinitiator).

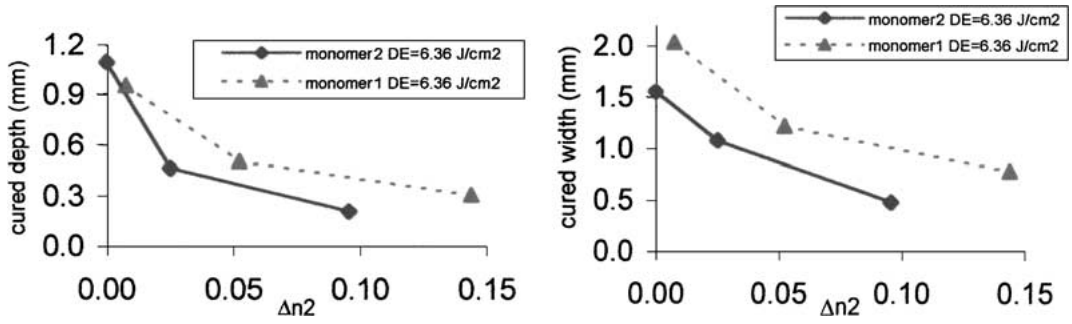

Figure 6 Cured depth and width function of the squared refractive index difference between powder and monomer.

(0.6 μm, 1.5 μm, 2.9 μm and 4.4 μm), using three densities of energy (Fig. 5).

Whatever the density of energy, the variation of cured depth follows a linear law with the mean diameter of particles, that are in agreement with Equations 1 and 3. Cured width also follows a linear law in function of the mean particle diameter, with slopes also depending on density of energy.

3.6. Influence of the refractive index difference between the powder and the monomer

The influence of the refractive index difference between the powder and the monomer was evaluated by using alumina ($n = 1.7$), silica ($n = 1.5$) and zircon ($n = 1.85$) powders and the two monomers given in Table I. Fig. 6 gives the measured cured depth and width in function of $\Delta n^2 = (n_{\text{powder}} - n_{\text{monomer}})^2$. The cross sectional dimensions of a cured line are decreasing when the difference of refractive index between powder and monomer is increasing. It is difficult to obtain a real tendency for cured depth and width in function of Δn^2. The cured depth does not follows a linear law in function of $d_{50}/\Delta n^2$ as suggested by Equations 1, 3 and 4.

3.7. Dimensionnal resolution

Width and depth of polymerization rules the dimensionnal resolution but also the physical properties of the green piece (homogeneity, curing shrinkage, adhesion between layers, ...). The dimensional resolution of the CT1200SG alumina system has been studied by varying the density of energy and the layer thickness. Two scanning patterns have been tested: a first one with single lines parallel to the spread axis (Fig. 7), and a second one representing a mesh pattern (parallel and perpendicular lines to the spread axis) of 1 and 2 mm (Fig. 8). In the case of single lines of 10 layers of 25 μm depth, a limit resolution of 170 μm was reached for an energy density of 30 mJ $\cdot$ cm^{-2} (Fig. 7). This density of energy represents the lowest one for which satisfactory adhesion between layers was obtained in order to avoid pull out during deposition of the subsequent layer.

In the case of the mesh pattern, the limit resolution reached was about 230 μm, with a hole diameter of about 600 μm.

Dimensionnal resolution is increasing with the decrease of the density of energy applied to the paste (cured width is lowered). But there is a limit value of density of energy for which adhesion between layers (and so, cured depth) is not strong enough to avoid pull out of the cured shape, when a new layer is spread. This limit value of density of energy depends on several parameters, such as spreading parameters (shear stress), layer thickness and UV reactivity of the paste.

3.8. Mechanical characterisation

An average value of 275 MPa is obtained for as-sintered alumina samples. This value is similar to that of pressed alumina specimens, i.e., 265 MPa. It is then possible to fabricate complex shape parts by stereolithography with similar mechanical properties than those obtained by classical shaping process like uniaxial pressing.

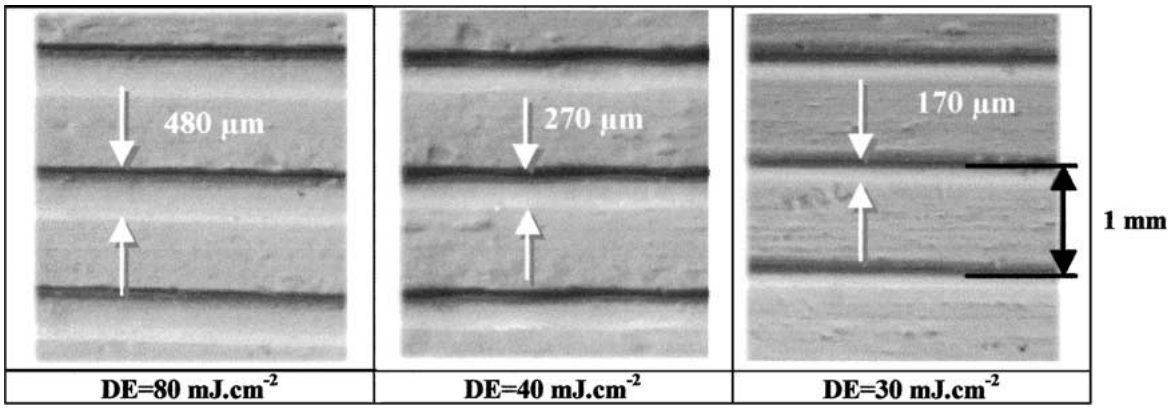

Figure 7 Cured lines for different densities of energy (spacing 1 mm, layer thickness 25 μm, 10 layers).

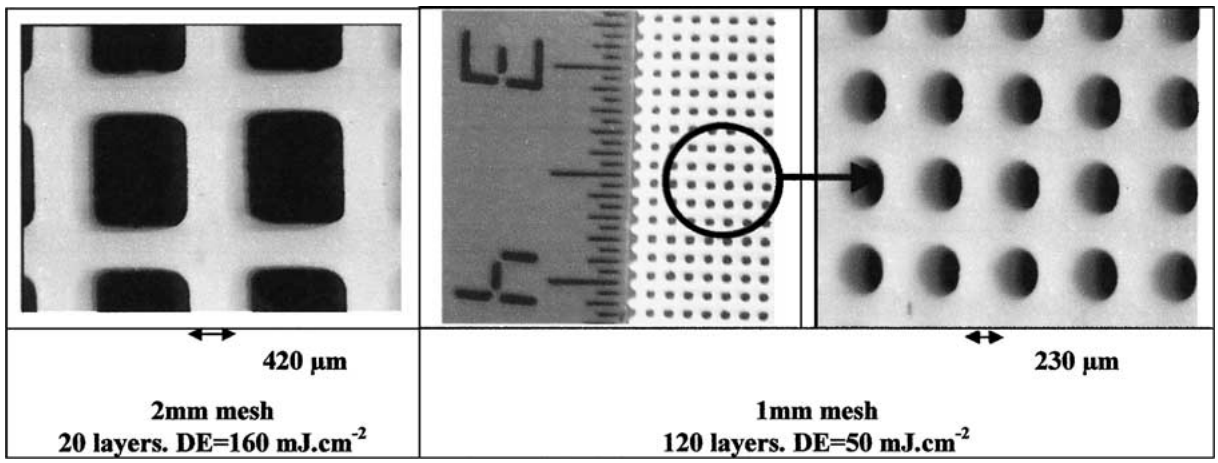

Figure 8 Mesh patterns for two densities of energy, layer thickness 25 μm.

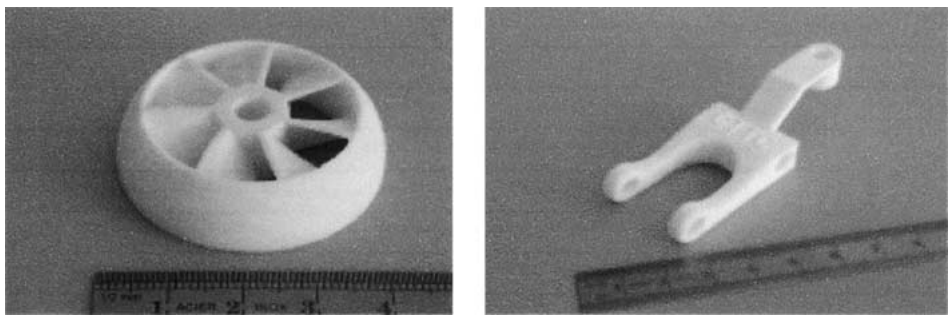

Figure 9 Examples of alumina (CT1200SG) sintered pieces elaborated by stereolithography.

3.9. Examples of sintered ceramic parts obtained by stereolithography

Two examples of alumina (CT1200SG) sintered pieces elaborated by stereolithography process are shown in Fig. 9.

4. Conclusion

The major drawback of the fabrication of complex shape ceramic parts is the cost of the mould, the difficulties to obtain different complicated cross sections and the processing time required to develop the first prototype.

Rapid prototyping offers an unique opportunity to fabricate, without using costly moulds, complex ceramic parts with mechanical properties similar to those obtained by classical processing routes, in a very reduced time.

A key point is the definition of a suitable photocurable paste, which has to fulfil many requirements in terms of rheological behaviour, and in terms of UV reactivity. A formulation containing a high concentration of ceramic particles (60 vol%) and reactive to UV radiation (depth of polymerization larger than 200 μm) has been defined with a rheology adapted to the process. Dimensional tolerances of $\pm 0.5\%$ can be achieved on some centimetres size sintered pieces with a good choice of experimental parameters (radiation energy, scanning speed. . .).

References

1. C. HINCZEWSKI, S. CORBEL and T. CHARTIER, *J. Eur. Ceram. Soc.* **18** (1998) 583.
2. *Idem.*, *J. Rapid Prototyping.* **4**(3) (1998) 104.
3. M. L. GRIFFITH and J. W. HALLORAN, *J. Amer. Ceram. Soc.* **79**(10) (1996) 2601.

4. H. LIAO and T. W. COYLE, *J. Canadian Ceram. Soc.* **65**(4) (1996) 254.
5. G. A. BRADY, T. M. CHU and J. W. HALLORAN, in Proceedings of the Solid Freeform Fabrication Symposium (University of Texas, Austin, 1996) p. 403.
6. M. L. GRIFFITH, T. M. CHU, W. C. WAGNER and J. W. HALLORAN, in Proceedings of the Solid Freeform Fabrication Symposium (University of Texas, Austin, 1995) p. 31.
7. C. HINCZEWSKI, PhD Thesis, Institut National Polytechnique de Lorraine, France, 1998.

Received 3 June
and accepted 1 October 2001